Selective Benzyl Alcohol Oxidation over Pd Catalysts

Carine Edith Chan-Thaw [1] , Aditya Savara [2],* and Alberto Villa [3],*

1   Institut pour la Maîtrise de l'Énergie, Université d'Antananarivo, BP 566, Antananarivo 101, Madagascar; carine.chanthaw@gmail.com
2   Chemical Sciences Division, Oak Ridge National Laboratory, Oak Ridge, TN 37831, USA
3   Dipartimento di Chimica, Università degli Studi di Milano, via Golgi 19, 20133 Milano, Italy
*   Correspondence: savaraa@ornl.gov (A.S.); alberto.villa@unimi.it (A.V.); Tel.: +1-865-576-6311 (A.S.); +39-02-5031-4361 (A.V.)

Abstract: In the last decades, the selective liquid phase oxidation of alcohols to the corresponding carbonyl compounds has been a subject of growing interest. Research has focused on green methods that use "clean" oxidants such as O_2 in combination with supported metal nanoparticles as the catalyst. Among the alcohols, benzyl alcohol is one of the most studied substrates. Indeed, benzyl alcohol can be converted to benzaldehyde, largely for use in the pharmaceutical and agricultural industries. This conversion serves as model reaction in testing new potential catalysts, that can then be applied to other systems. Pd based catalysts have been extensively studied as active catalytic metals for alcohol oxidation for their high activity and selectivity to the corresponding aldehyde. Several catalytic materials obtained by careful control of the morphology of Pd nanoparticles, (including bimetallic systems) and by tuning the support properties have been developed. Moreover, reaction conditions, including solvent, temperature, pressure and alcohol concentration have been investigated to tune the selectivity to the desired products. Different reaction mechanisms and microkinetic models have been proposed. The aim of this review is to provide a critical description of the recent advances on Pd catalyzed benzyl alcohol oxidation.

Keywords: palladium; benzyl alcohol; oxidation

1. Introduction

The interest in the selective liquid phase oxidation of alcohols to the corresponding carbonyl compounds (aldehydes or ketones) has been intensifying continuously [1–5]. Many homogeneous palladium catalysts have been reported [6,7] but besides the difficulty to isolate the catalyst from the reaction mixture, reusability of expensive noble metal and purification of products remain a complex task. Noble metal heterogeneous catalysts represent thus a valid alternative due to the easier catalyst recycling and products separation [1,8].

Among these alcohols of interest, benzyl alcohol (BA) is one of the most studied substrates. Benzaldehyde that results from the selective oxidation of BA is an industrially practical intermediate molecule in the pharmaceutical, fragrances and agricultural industries industries [9,10]. Depending on the catalytic materials and the reaction conditions (temperature, solvent, oxygen pressure), many products of industrial interest, such as benzaldehyde, benzyl benzoate, benzoic acid and benzyl ether can be obtained [11]. For example, benzaldehyde is used as flavoring agent and as precursor for the production of pharmaceuticals to plastic additives [12–14]. Benzyl benzoate finds applications as topical treatment for human scabies, as well as dye carrier [15]. BA oxidation has been carried out in organic solvents such as toluene, diethoxyethane, dimethyl sulfoxide (DMSO), dimethylformamide (DMF), [16–19] though such processes can produce undesired organic wastes. Conventionally,

stoichiometric strong oxidants known to be toxic and expensive are utilized [20–22]. Both parameters, solvent and oxidants, led therefore to environmental concerns and motivation for developing alternative catalytic processes. Research has consequently focused on green methods that use "clean" and cheap oxidants such as O_2 in combination with supported metal nanoparticles as the catalyst for the solvent-free aerobic oxidation of alcohols [1,8].

Several supported noble metal nanoparticles catalysts (e.g., Pt, Pd Ru and Au NPs) have been investigated to increase both the BA conversion and the benzaldehyde selectivity with molecular oxygen or hydrogen peroxide [1,2,8]. Among them, Pd based catalysts have particularly been extensively studied as active catalytic metals for alcohol oxidation for their high activity and selectivity to the corresponding aldehyde [23–27]. The addition of a second metal to Pd, in particular Au, to form bimetallic systems have been shown to modulate the activity, selectivity and durability of the catalyst [28–30] The catalytic activity of such noble metal nanoparticles is dependent on their size, shape/morphology, valence and physicochemical properties [31]. These characteristics of the NPs are controlled partly by the catalyst support, when one is used. As will be described, some information has been obtained regarding the possible active sites and several research groups focused on the rational design of morphology and size-controlled nanostructures.

The catalytic activity, selectivity and stability is also tuned by the support properties. Stability of the NPs could take place thanks to the metal support interaction and thanks to the beneficial effect of a polymer protective agent for the supported Pd NPs. Indeed, restructuring and leaching of metal NPs often arise in liquid phase reaction and outcome to the deactivation of the catalyst [32]. The dissolution of the support material can also occur during liquid phase reactions. Because of all these limitations and concern in increasing the activity and selectivity, the design of active and resistant materials is still a challenge.

This review aims at providing a fairly broad description of what has been learned so far towards designing the ideal catalyst for the BA oxidation. Some studies have conflicting results and we have attempted to present a balanced view of the current understanding. The importance of the shape and the size of Pd NPs will be described before discussing about the potential advantages of using a gold palladium alloy to perform this reaction. Subsequently, the importance of the reaction conditions will be described, along with the mechanism and microkinetics of the reaction network.

2. Pd Morphology

Supported Pd nanoparticles have been extensively reported active and selective to benzaldehyde in the BA oxidation. To understand and enhance these catalytic performances, the effects of size and morphology of these metal nanoparticles have been studied. Size, shape and morphology can be modified by the preparation method, the use of a protective agent and a reductive agent. Moreover, when a second metal is added to Pd, the final structure (alloy, core-shell, etc.) strongly influences activity and selectivity.

2.1. Pd Size/Shape

Different studies indicated that the size of the metal nanoparticles is a key factor in determining the catalytic activity and selectivity in the aerobic oxidation of alcohols. However, very few reports have investigated the particle size effect in the aerobic oxidation of alcohols, in particular for Pd catalyzed BA. Li et al. [33], compared the catalytic behaviors of Pd supported on NaX zeolite catalysts with different mean sizes of Pd for the oxidation of benzyl alcohol. Among the catalysts in that study, Pd with mean size of 2.8 nm exhibited the highest conversion, while the catalysts with both larger and smaller Pd particles showed lower conversions Figure 1.
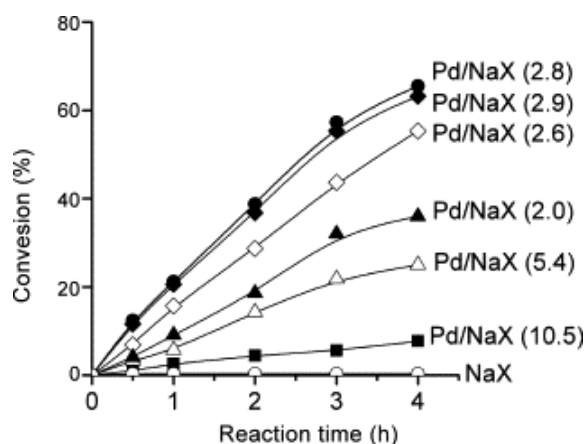
Figure 1. Conversions of benzyl alcohol versus reaction time over the 1.35 wt% Pd/NaX catalysts with different mean sizes of Pd particles. The mean size of Pd (in nm) was shown in the parenthesis. Reprinted from ref. [33]. Copyright 2008, with permission from Elsevier.

The authors also calculated the intrinsic turnover frequency (TOFs) (i.e., mols of substrate converted at the initial stage per mole of surface Pd per hour) using the initial conversion rate and the Pd dispersion evaluated by CO chemisorption. They concluded that the intrinsic TOF depends significantly on the mean size of Pd particles, confirming that the catalyst with a mean size of Pd of 2.8 nm is the most active. Similar highest activity size ranges have been found by other authors. Chen et al. prepared a series of Pd/SiO$_2$-Al$_2$O$_3$ tuning the Pd mean particles size from 2.2 nm to 10 nm [34]. At a size of 3.6–4.3 nm, the highest value of intrinsic TOF, that is moles of BA converted per mole of surface Pd per second, was calculated from the experimental data (Figure 2).
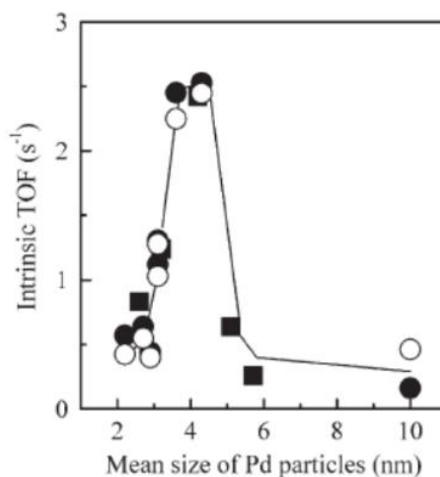

Figure 2. Dependence of the intrinsic turnover frequency on the mean size of Pd particles. The catalysts were reduced either by hexanol (full square) or H$_2$. In the case of H$_2$, the TOF was either based on Pd dispersion estimated by mean size of Pd (full circle) or based on Pd dispersion evaluated by CO chemisorption (empty circles). Reprinted with permission from ref. [34]. Copyright 2008 WILEY-VCH Verlag GmbH & Co. KGaA, Weinheim.

The key role played by both the Pd NPs size and the Pd NPs distribution in the activity and selectivity to benzaldehyde was also investigated by Zhou and coauthors [35]. Pd was loaded on covalent organic polymer with a DMF (Pd/COP-4-DH) or aqueous (Pd/COP-4-WH) solution of palladium and reduced under H$_2$. Pd/COP-4-DH with a mean Pd size of 7.7 nm and a dispersion of 0.145 was more active in the BA oxidation at 160 °C than Pd/COP-4-WH with its 9.9 nm and 0.113 dispersion (32% conversion and 95411 h^{-1} TOF vs. 20.1% conversion and 65,924 h^{-1} TOF for

Pd/COP-4-DH and Pd/COP-4-WH, respectively). The catalytic performance reported is a bit higher than other studies but we would like to draw attention to the differences observed in selectivity. Pd/COP-4-DH with its smaller Pd NPs is less selective (57.1%) than Pd/COP-4-WH (89.8%), with Pd/COP-4-DH having a broader particle size distribution. Evidently, the particle size also affects the selectivity. In this size range, the changing of the particle size can also result in changes in the types of sites present. It is likely that the necessity of the optimal Pd mean size reveals the need of a pertinent ratio of the edge and corner Pd atoms to the terrace Pd atoms.

Further studies have shown that the selectivity toward each product is related to the presence of specific active sites [36] but also to the adsorption geometry and orientation of reactants and products [37]. In situ attenuated total reflection infrared (ATR-IR) spectroscopy combined with site selective blocking by CO allow to discriminate the different sites involved in the liquid-phase oxidation of BA on Pd/Al$_2$O$_3$ [36,38,39]. Ferri et al. [36] showed that the oxidative dehydrogenation of the alcohol to benzaldehyde, showed only little dependence on structure and occurred on all exposed Pd faces, whereas benzene, an undesired product deriving from decarboxylation occurred preferentially on hollow sites on Pd (111) planes. Different strategies have been adopted to avoid the formation of undesired products. For example, after the addition of Bi to Pd/Al$_2$O$_3$, the catalyst showed no adsorbed CO during dehydrogenation, suggesting that the sites on Pd(111) planes are blocked by selective deposition of Bi [40]. Our group showed that the utilization of polyvinylalcohol (PVA) capped Pd nanoparticles supported on Al$_2$O$_3$ enhanced selectivity to benzaldehyde in the liquid phase BA oxidation, by limiting the decarbonylation reaction [38]. Using diffuse reflectance infrared spectroscopy (DRIFTS) and by monitoring the adsorption of CO as the probe molecule we have shown that PVA is preferentially absorbed on the 111 plane, based on attenuation of the signal at 1945 cm^{-1} peak for the Pd$_{PVA}$ sample (Figure 3). The removal of PVA by mild calcination completely restored the signal at 1980 cm^{-1} in DRIFT spectra, associated to the μ_2 bridge-bonded CO on Pd (100), which was shifted to 1960 cm^{-1} for Pd$_{PVA}$ NPs. In contrast, the signal at 1925 cm^{-1}, ascribed to the perturbation of CO coordination on (111) plane, has a low intensity even after calcination, thus indicating a stronger interaction of PVA with Pd (111) facets. These studies show (in contrast to some studies) that not only is BA oxidation structure sensitive but that it is possible to tune the selectivity based on knowledge of how the structure is correlated with the selectivity.
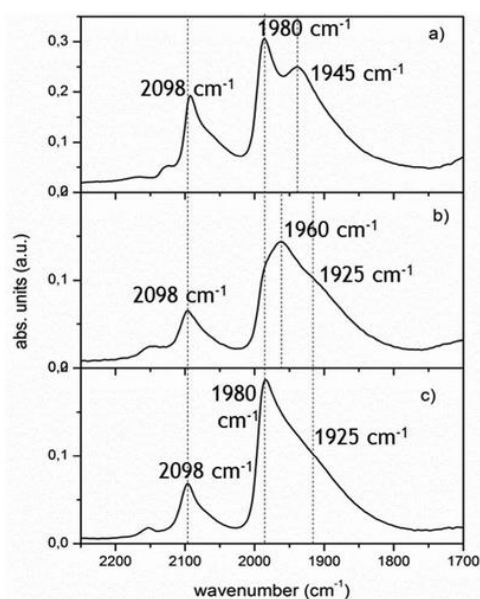
Figure 3. Diffuse reflectance infrared (DRIFT) spectra of adsorbed CO on (**a**) 5 wt.% Pd/Al$_2$O$_3$, (**b**) 5 wt.% Pd$_{PVA}$/Al$_2$O$_3$ and (**c**) calcined 5 wt.% Pd$_{PVA}$/Al$_2$O$_3$. Reprinted with permission from ref. [38]. Copyright 2016, with permission from American Chemical Society.

2.2. Bimetallic Catalysts

Studies have shown that the selectivity and activity can be modulated by addition of a second metal to Pd. In particular, it has been reported that the addition of Au to Pd can alter the catalytic activity, selectivity to benzaldehyde and durability of the catalyst in the BA oxidation [28–30,41–45]. Whether this alloying increases or decreases the activity and selectivity towards the aldehyde product varies between studies and is still not completely understood. It is possible that the support plays a role in which effect the alloying of Au has. Prati's group was among the first to demonstrate that the presence of AuPd alloy supported on activated carbon showed similar catalytic activity to the monometallic Pd (TOF of 38 to 54 h cm^{-1}, for Pd and AuPd, respectively), while giving a greater selectivity (>94%) to benzaldehyde [28]. The slightly higher activity observed for AuPd in that study has been ascribed to a geometric effect. Indeed, in AuPd the interatomic distances, are different than in the pure metals. AuPd alloys did not only show a higher activity than Pd but also a better resistance to deactivation, limiting the leaching of the metal and deactivation by O_2 poisoning [46,47]. Using the same preparation method, it was demonstrated the general applicability of single phase alloy with Au/Pd molar ratio varied from 9:1 to 2:8. The best performance being obtained when uniformly mixed alloyed bimetallic nanoparticles were prepared (Au/Pd range 9:1−6:4), among which Au_8-Pd_2/AC was most efficient [48]. The higher activity of Au-rich catalyst has been attributed to the formation of uniform Au-Pd alloy, whereas in the case of Pd-rich segregation of the Pd nanoparticles and inhomogeneity in the alloy structure has weakened the synergistic effect.

Hutchings' group extensively studied the effect of AuPd morphology, in particular when supported on TiO_2 [29]. High activities were detected, with TOFs values that increased from 14,270 h^{-1} to 86,500 h^{-1}, increasing the reaction temperature from 383K to 433K. The high activity was attributed to the formation of an Au-rich core/Pd-shell structure, with an electron promotion effect for Au on Pd.

Other studies also showed that the addition of Au to Pd increases also the selectivity to benzaldehyde, depressing the formation of toluene, main side product formed in this reaction [49,50]. The effect of Au:Pd ratio has been investigated and it was determined that AuPd 1:1 weight ratio produced the highest catalytic activity [51]. In these studies, the Pd-rich catalysts showed a selectivity of 66−70% to benzaldehyde with the formation of 21% of toluene as side-product, whereas Au-rich catalysts yield to 95% of benzaldehyde, depressing the formation of toluene. The effect of Au-Pd ratio has been successively studied by Silva et al. [52].

In this work, the authors observed a volcano-type behavior and the highest catalytic activity was observed for Au:Pd 10:1 molar ratio (Figure 4). In this study, the Au Pd ratio did not have a significant influence on the selectivity of the reaction (Figure 4). High-angle annular dark-field scanning transmission electron microscopy (HAADF-STEM) studies showed bimetallic nanoparticles with Au-rich core and Pd-rich shell structure. The Au-Pd system with 10−1 molar ratio corresponds to the composition required to the complete coverage of Au cores with one atomic layer of Pd [52]. Using density functional theory calculations, the authors concluded that the enhanced activity of this system (Au:Pd 10:1) is a balance between the number of activity sites and the rate of product desorption. For Pd content lower than 10% the low activity was attributed due to a lower adsorption of BA. For Pd content higher than 10%, the calculations suggested an increased BA adsorption and a higher energy for desorption of benzaldehyde. In contrast to the results by Silva, Baiker's group, for example, reported the synthesis of tetrakis-(hydroxymethyl)-phosphonium chloride (THP) protected AuPd nanoparticles supported on PANI varying the AuPd ratio from 7−1 to 1−9 [16]. Interestingly, in contrast to the previous studies, the highest activity has been achieved using a Pd-rich catalyst (Au:Pd 1−9). Moreover, in the study by Baiker, the AuPd ratio has an influence on the selectivity to benzaldehyde, which decreased by increasing the Au content, probably due to the formation of benzoic acid. The decrease in activity and selectivity observed by Baiker are consistent with results by Villa et al. [53].
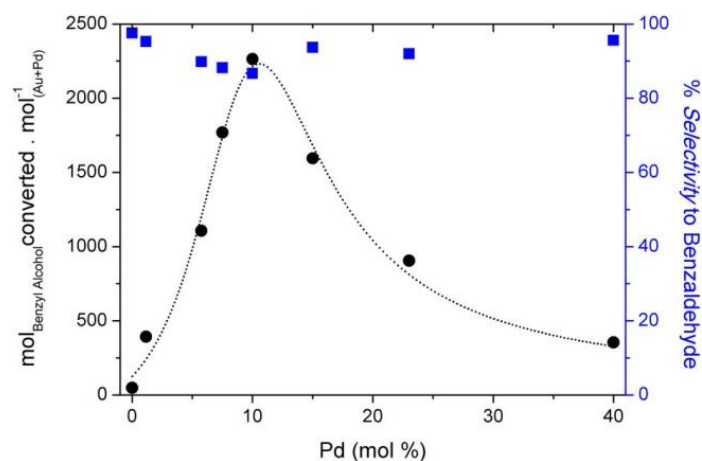
Figure 4. The effect of Au-Pd ratio in the benzyl alcohol oxidation. Reproduced with permission from ref. [53] under a Creative Commons Attribution-NonCommercial-NoDerivs 4.0 International License, as described at https://creativecommons.org/licenses/by-nc-nd/4.0/legalcode.

Clearly, the composition of AuPd particles are not the only factor. The effect of AuPd morphology (alloy versus core-shell structure) has also been investigated [47,54]. AuPd nanoparticles were synthesized in the presence of PVA as stabilizer by co-reduction of the two metals, resulting in the formation of pure AuPd alloy (Au + Pd) [47]. Separately, the, sequential reduction of Au and Pd, or vice versa, resulted in the formation of core-shell structures (Au@Pd and Pd@Au, respectively) (Figure 5) [54].
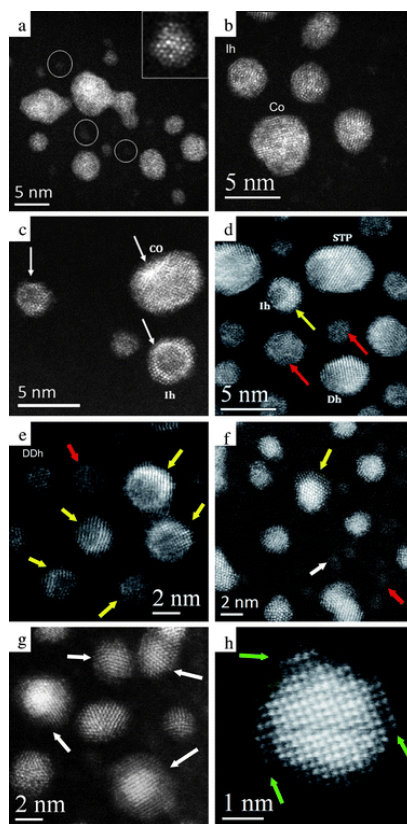
Figure 5. STEM HAADF images of the (**a**,**b**) (Au + Pd); (**c**,**d**,**e**) (Au@Pd) and (**f**,**g**,**h**) (Pd@Au). Republished with permission of Royal Society of Chemistry from ref. [56]; permission conveyed through Copyright Clearance Center, Inc. The original work associated with the image is available online at https://doi.org/10.1039/C1FD00020A.

The morphology of the catalysts had a significant effect on the catalytic activity and the most active catalyst was the Au_{core}-Pd_{shell} catalyst but it did not have the best selectivity towards the aldehyde product. In these studies, calcination treatment has been performed (673K in air) in order to remove the PVA from the metal surface and to investigate the effect of PVA on the catalytic performance has been investigated [47,54]. The high temperature used efficiently removed the PVA form the surface but affecting the morphology of the catalyst, with a general growing of the AuPd particles, more evident in the activated carbon supported ones. As a consequence, all the catalysts resulted less active than untreated one.

As in earlier studies with Bi, deposition of Bi on the surface of AuPd nanoparticles can further improve the selectivity to benzaldehyde (95% and 88% for BiAuPd and AuPd, respectively) by suppressing the formation of toluene [55]. The effect was ascribed to the blocking of specific active sites of AuPd responsible of the undesired reaction after Bi deposition. However, additional experiments are required to probe possible electronic effects.

2.3. Support Effect

The Pd and AuPd studies showed that size and morphology are not the only factors involved. Different studies showed that the support has a role on the catalytic performance of metal nanoparticles in particular in the liquid phase reaction [56,57]. From surface science, it is known that the support properties can influence the interaction with the metallic particles, potentially modifying both their electronic and structural properties. For example, the presence of heteroatoms on the carbon surface can provide different anchoring sites for the nanoparticle, increasing the stability of the nanoparticles during the reaction [58]. Catalyst deactivation is mainly due to metal leaching, overoxidation, sintering or irreversible adsorptions [8]. On the other hand, base functionalized surfaces can favor H-abstraction, effectively speeding up the oxidative dehydrogenation of alcohols [8]. The real contribution of the support is still under debate and much effort should be paid to understand its effect. Metal oxides such as SBA-15 [59], MCM-41 [60], alumina [61] and carbonaceous materials [58] with different morphology and functionalization have been used as support. In this section, we will be report selected examples of attempts to elucidate the effects of supports on activity, selectivity and durability.

2.3.1. Oxides

He et al. [62] deposited Pd by a modified deposition-precipitation approach on hydrotalcite and obtained an active (TOF value of 5330 h^{-1}) and stable catalyst for the BA oxidation. The utilization of a basic support is believed to speed up the reaction, facilitating the H-abstraction and these activities are higher than many studies even though they are not the highest activities reported. Using an adsorption method, Qi and coauthors [63] prepared Pd nanoparticles (1 wt.%) supported on MnO_x for the solvent-free BA oxidation at 120 °C, labelled as Pd/MnO_x-ads. When Pd/MnO_x-ads was further reduced under H_2, the material was labelled Pd/MnO_x-ads-H; whilst when prepared by co-precipitation the sample was labelled Pd/MnO_x-cp. After 5 hours of reaction, 69.5% of conversion was obtained using Pd/MnO_x-ads versus 59.5% and 65.3% for Pd/MnO_x-ads-H and Pd/MnO_x-cp, respectively. Mn_3O_4, CeO_2 and Fe_2O_3 were also used as support for comparison. When comparing these catalysts, activity of the corresponding Pd supported catalysts, Pd/Mn_3O_4-ads, Pd/CeO_2-ads, Pd/Fe_2O_3-ads was lower than the one obtained with Pd/MnO_x-ads. The difference of support played a role in the average mean Pd sizes as well as distribution. These results point to the fact that the support does not only affect the electronic properties of the catalytic metal particles but also the size morphology and stability.

Ordered mesoporous structures, namely SBA-15 and MCM-41, were prepared by Karimi et al. in refs [59] and [60] respectively. SBA-15 has a regular channel structure and SBA-15 with pore diameter of 7.6 nm were used to study the aerobic oxidation of BA in toluene at 80 °C. Pd/SBA-15 (0.4 mol%) which was functionalized with a bipyridylamide ligand was highly active and selective (over 99% yield of benzaldehyde) after five hours. The second structure, MCM-41 was also active

for the solvent-free aerobic oxidation of BA. The authors prepared a series of Pd supported MCM-41 with varying synthesis parameters. In one preparation, after the addition of Pd, the sample was further Soxhlet-extracted with a solution of acidified ethanol and dried at 80 °C for 24 h; the obtained catalyst was labelled Pd-M41-AE. When the sample was calcined at 550 °C instead of simply dried the sample was denoted Pd-M41-AC. In a third preparation, MCM-41 surface was functionalized with 3-aminopropyltrimethoxysilane before the addition of Pd and those catalysts were labelled Pd-AP-M41. The catalyst which was Soxhlet-extracted with an acidified ethanol solution, Pd-M41-AE, was the most active of the series (33.8% BA conversion and a TOF of 4344 h^{-1} with a Pd loading optimized at 0.4 wt.%, after one hour) for the BA oxidation mostly due to the smaller Pd NPs size (7.1 nm and 12.5 nm for Pd-M41-AE and Pd-M41-AC, respectively). For the same Pd loading, Pd-AP-M41 and Pd-M41-AC exhibited a conversion of 0.8% (TOF of 2095 h^{-1}) and 16.3% (TOF of 103 h^{-1}), respectively. This could mainly be attributed to the smaller Pd particles in Pd-M41-AE. These studies suggested that the pores of the support can play a role, in addition to the chemical interaction of the support. Likewise, 1 wt.% Pd supported on nanofiber-like mesoporous alumina prepared by sol immobilization method was reported as an effective catalyst for the BA oxidation [64]. Pd NPs could be stabilized by the support and the catalyst was revealed to be more active than the counterparts Pd/γ-Al$_2$O$_3$ and Pd/SBA-15 under the same reaction conditions. This performance is interpreted as being due to the combination of greater accessibility of active surface Pd species and potentially better metal support interaction.

A nanoporous CeO$_2$ support was investigated by Wang et al. [65], with loading of 1 wt.% Pd species on a crystalline nanoporous CeO$_2$, followed by testing the material for the aerobic BA oxidation under solvent-free conditions. Macroscopically observable activity (82.1% BA conversion) was observed, with noteworthy selectivity to benzaldehyde (97.6%). The results were explained by the synergistic effects between abundant nanopores and weak adsorption of the molecules on CeO$_2$ but further investigation is merited to isolate the chemical and structural factors.

More innovative support structures have also been investigated in an attempt to find unconventional ways of improving the catalytic performance of Pd NPs. Titanate nanobelts were investigated as support for Pd NPs for the same reaction [66]. Pd NPs were immobilized on the uncalcined and calcined titanate nanobelts by polyol reduction and tested at 120 °C in an oil bath under continuous oxygen stream. After one hour of reaction, Pd immobilized on calcined titanate nanobelts (2.17 wt.% Pd/TNB) exhibited macroscopic activity (45.2% versus 30.2% for the calcined and uncalcined support, respectively) and high selectivity to benzaldehyde (98.5% versus 88.4% for the calcined and uncalcined support, respectively) without any formation of toluene compared to the Pd loaded on the uncalcined support (2.6 wt.% Pd/TNB-u). The higher activity and selectivity of Pd/TNB is explained by the basic nature of titanate nanobelts formed after calcination. Indeed, after the total removal of water, partial hydrolysis and Na$^+$ exchange in titanate nanobelts could be totally restrained and therefore intensify the basicity of the support.

In addition to efforts to study the support, efforts have also been made to modify the supports' surface by addition of functional groups, typically to increase the metal-support interaction. Chen et al. [67] incorporated nitrogen heteroatoms inside the mesoporous molecular sieve SBA-15 which acted as support for the Pd NPs. The obtained catalyst prepared by sol immobilization and denoted 2 wt.% Pd/SBA-15-900 N (where 900 stands for the nitridation temperature in Celsius), was tested in the solvent-free aerobic oxidation of BA at 120 °C. Thanks to the terminal $-$NH$_x$ species, a better dispersion of the 2 wt.% Pd NPs was obtained leading to the good catalytic performance (63.0% conversion and 93.3% selectivity to aldehyde) and sufficient stability for over 5 runs. In another study, a different chemical modification of SBA-15 was performed by the addition of Zr. Compared to the pure SBA-15, the acidic sites of the platelets ZrSBA-15 (Zr/Si = 0.05) are amplified favoring thus the interaction between Pd NPs and ZrSBA-15 as reported by Ji at al. [68]. This better metal-support interaction led therefore to a well-organized dispersion of Pd NPs. The 3.3 wt.% Pd/ZrSBA-15 was prepared by adsorption-deposition method and an average Pd NPs size of 1.9$-$2.3 nm was obtained.

The catalyst was tested at 90 °C for 4 h and mainly benzaldehyde was detected. Pd/ZrSBA-15 resulted in an active, selective and stable catalyst over 5 runs. To further increase the metal support interaction, it was thought that the Zr and N chemical modifications of the support could be used with a synergistic effect to increase the recycling performance of Pd/ZrSBA-15, so the same authors introduced a coating of N-doped carbon inside the acidic ZrSBA-15 support with short pore channels [69]. The combination of both the anchoring sites of N-doped carbon and the acidic framework of the inorganic support ZrSBA-15 led therefore to better dispersion of the Pd NPs inside the pore channels of the resulting platelets-like N-doped carbon ZrSBA-15 support. The catalyst maintained catalytic activity (82% conversion) and selectivity to benzaldehyde (99%) after ten cycles.

In other studies, chemical modifications were made on magnetic supports. The magnetic supports may not be superior supports for Pd NPs but they can enable facile catalyst separation and recycling from the post-reaction solution. Pd NPs supported on Fe_3O_4/amino acid nanocomposite was demonstrated as a highly active magnetic catalyst for the reaction of interest at 50 °C [70]. The best activity and stability over 7 runs were attained when cysteine was used as the amino acid to form the catalyst Fe_3O_4/cysteine-Pd NPs. The authors ascribed the results, compared to the other selected amino acid, to the presence of the sulfur groups in the cysteine structure. The idea of using a magnetic support was also utilized by Kong et al. [71]. The authors prepared a core-shell structure multifunctional $Pd/Fe_3O_4@mCeO_2$ nanocatalyst and the catalyst result active, selective to aldehyde and stable during the selective oxidation of BA. They explained the performance by both the Fe_3O_4 core which allows the magnetic driven separation and recycling catalyst and the defect-rich CeO_2 shell that enhances the catalytic properties of the loaded Pd NPs.

2.3.2. Carbon

Because of their high surface area, good chemical stability and easy recovery of noble metals, carbon materials have attracted attention as the common catalyst support for noble metal. There are several the carbon supports: activate carbon (AC), carbon nanotubes (CNT) and graphenated carbon (GC). Recently, BA oxidation was carried out at 110 °C with the same Pd loading (about 0.7 wt.%) to compare these supports and GC had the highest activity (30,137 mol/h mol_{Pd}, 11,267 mol/h mol_{Pd} and 6910 mol/h mol_{Pd} for Pd/GC, Pd/AC and Pd/CNT, respectively) [72]. The authors interpreted these results as meaning that the π-electron interaction between the aromatic group and graphene resulted in a higher adsorption of reactant alcohol and oxygen promote undeniably the aerobic oxidation reaction, a concept that has also been reported for aromatics on hydroxyl groups [73]. Another study reported that Pd NPs supported on graphene nanocomposite achieved selective oxidation of BA with 100% conversion and over 99% selectivity to benzaldehyde [74].

As with other supports, groups have attempted to increase the support metal interactions of carbon supports by chemical means. GC functionalized with oxygen atoms (OH and COOH groups), also referred to as graphene oxide, was studied in the context of a graphene oxide (GO) nanocomposite, with a nonionic triblock copolymer (Pluronic 123) and Pd NPs [75]. The so-obtained Pd-GO/P123 was revealed an active nanohybrid material for the BA oxidation. Adding the surfactant P123 prevented the self-assembly and aggregation of Pd-GO, enhanced both the Pd-GO dispersity and oxygen solubility in aqueous media. CNTs have also been modified chemically to increase better interactions with metal particles. Because the adsorption of Pd on both N- and B-doped carbon support showed better interactions with a supported metal compared with an undoped carbon support, palladium-supported boron-doped hollow carbon spheres were synthesized for the solvent-free aerobic oxidation of BA [76]. The higher activity of the B-doped carbon support is ascribed to the high Pd NPs dispersion and the accessibility of the reactant to the catalyst. Boron assists both in binding to the Pd by inducing strong B-Pd bonds and improving the stability of the hollow carbon sphere towards oxidation.

Several other studies demonstrated the appreciable results obtained by the introduction of N heteroatoms into the carbon supports [24,25,50,77–79]. These authors immobilized Pd NPs prepared with the use of PVA sol on three different N containing carbon supports (covalent triazine framework (CTF), N-CNTs and CNTs) and on a commercially available AC support [24]. In this study, high percentages of N heteroatoms (9 wt.%), followed by Pd NPs supported on CTF exhibited similar initial activity but better stability as compared to Pd/N-CNTs with 2 wt.% N. Activity and stability of the CTF based catalyst during the BA oxidation are ascribed to the N heteroatoms. In the same family of hybrid porous solids as supports, microporous covalent organic polymer (COPs) have also attracted consideration because not only of their hydrothermal stability but also to their moderately stable covalent C−C, C−H and C−N bonds (that is, built-in chemical functionality) [35]. Due to the N heteroatoms, Pd/COP synthesized by conventional impregnation and hydrogen reduction displayed high catalyst binding surface areas and allowed small Pd average particle size with a broad size distribution. The role of these N heteroatoms, including their locations, were then investigated by Chan-Thaw et al. during the BA oxidation [80]. The simple presence of N in proximity of the Pd NPs did not guarantee enhanced activity: the complexity lies in the N atoms not interfering with the Pd active sites. The access to specific Pd active sites is for example compromised when N species bind to Pd through the pyrrolic groups of the protective agent, PVP (as mentioned earlier). On the contrary, N groups covalently bound to the support typically positively impact the ultimate catalytic performance of Pd NPs, in part by reducing leaching of Pd NPs into the solution. The idea of controlling the morphology of Pd NPs was also studied by Arrigo et al. by nitrogen and oxygen functionalization of carbon supports [77]. The support was either functionalized with nitric acid HNO_3 (CNTox) that introduces mainly acidic oxygenated functionalities, or NH_3 (NCNT) that exhibits a broad distribution of O and N species. Polyvinyl alcohol was used as protective agent during the immobilization of the metal. The most desirable results were obtained with Pd/NCNT-600, where 600 °C was the temperature of the thermal treatment with NH_3. Given this ammonia treatment temperature, the derived stronger metal−N or metal−O bond at the interface prevented Pd NPs from sintering during reaction and enabled good catalytic performance. The performance and stability of Pd/NCNT in this reaction was also reported by Wang and coauthors [81]. In these studies, the selectivity to benzaldehyde was always over 90%: the successive oxidation of the aldehyde to carboxylic acid and also the subsequent esterification between BA and carboxylic acid were avoided.

For even high nitrogen contents, Pd nanoparticles have been also supported on ordered mesoporous carbon nitride (CN) and other carbon-based materials via impregnation by Xu et al. [82]. Thanks to the basic nitrogen sites, the ordered mesoporous CN allowed a superior dispersion of the Pd NPs as well as an easier activation of the alcohol molecules. The optimized amount of Pd was 4 wt.% on CN as more loading of Pd did not improve the BA conversion at 80 °C with toluene as the solvent. Moreover, the 4 wt% Pd/CN catalyst was relatively stable over five runs (all above 87% of conversion).

Composite materials have also been tested. A mixture of oxide and carbon support, that is manganese oxide-CNT composites [83] and organosilane-functionalised carbon nanotubes supports for Pd NPs were tested in the solvent-free selective oxidation of BA [84]. Three organosilanes groups were utilized and the authors reported that both the variety and number of surface-functional groups on CNT support affected the catalytic performance. By tuning the surface basicity surrounding the Pd NPs with the hydrophilic amino-containing (3-aminopropyl) triethoxysilane, it was possible to prepare small Pd particle size with narrow distribution, high electron density and an improved metal-support interaction.

While more work is required to fully understand the support effects, it is clear that carbon-based supports with nitrogen modification (or incorporation) appear to have a good balance between selectivity and stability.

3. Reaction Conditions

A full understanding of how the reaction conditions will influence the selectivity and the activity of the reaction requires knowledge of the mechanism in the kinetics, which will be discussed in Section 4. In this section, we summarize some of the results from the literature in a largely qualitative manner as, until recently, attempts to interpret the effects of the reaction conditions for benzylic alcohol oxidation over metal nanoparticles was done largely in the absence of a detailed reaction mechanism. The influence of the reaction temperature, the reaction time, the amount of catalyst, the BA concentration, the oxidant as well as the solvent on the catalytic activity had been investigated by various researchers. Early studies primarily used toluene as solvent [28]. However, after discovering that toluene may be formed during the reaction, different solvents, such as water, cyclohexane, xylene have been used [8]. This review will cover the results from non-protic solvents.

We first begin with summaries of what individual studies have observed, in this section of the review and discuss the kinetics and mechanism in more detail in Section 4. The detailed kinetics and mechanism in Section 4 are largely in agreement with the individual studies summarized in this section.

3.1. Temperature

The dependence of the activity and selectivity to the reaction temperature has been heavily studied, as temperature is typically a dominant factor in reaction kinetics and selectivity. As expected, the general trend is a higher conversion when increasing the reaction temperature. For example, Yang et al. have studied the effect of temperature using Pd supported on natural palygorskite (PG) as catalyst [85]. By changing the reaction temperature during the reaction in acetonitrile, the BA conversion increased (42%, 50% and 100% for 25, 40 and 60 °C, respectively) whilst the selectivity to benzaldehyde remained unchanged at almost the maximum (>99%) after 4 h. Other studies also showed relatively mild but significant effects of temperature on the reaction selectivity when using Pd particles at < 100 °C. Studies, performed using Pd/AC as catalyst, confirmed a trend of a decrease in selectivity to benzaldehyde when increasing the reaction temperature from 70 to 100 °C with the formation of a higher amount of toluene and benzyl ether (Figure 6) [86]. As will be described, in Section 4, kinetic modelling then suggested that this was because the activation barrier for the formation of toluene through the C−O bond cleavage is higher than for the benzaldehyde formation.

Study of the reaction temperature was also reported by Wu and coworkers [87]. In solvent-free reaction, the reaction temperature is increased compared to the reaction with a polar or non-polar solvent. 0.32 wt.% Pd/Al_2O_3 catalysts prepared by adsorption ($Pd/Al_2O_3\_ads$) or impregnation (Pd/Al_2O_3-imp) were evaluated both at 88 °C and 100 °C in the solvent-free oxidation of BA under O_2. Increasing the temperature from 88 °C to 100 °C, the reaction time was divided in two (8 and 4 h, respectively) for similar BA conversion, 97% and 83%, respectively for the $Pd/Al_2O_3\_ads$. This enhanced activity was more obvious with Pd/Al_2O_3-imp at 100 °C; 60% BA conversion was obtained in 4 hours compared to 8% after 8 hours at 88 °C.

The effect of reaction temperature on the selectivity has been studied using Au-Pd/TiO_2 catalyst [88]. Increasing the reaction temperature from 80 °C to 140 °C decreased the selectivity to benzaldehyde from 81% to 56% with the formation of a higher amount of toluene (16% and 40% at 80 and 140 °C, respectively). In further studies the same group showed that increasing the temperature from 80 °C to 120 °C decreased the selectivity to benzaldehyde from 92% to 75% whereas the selectivity to toluene increased from 9 to 27% [89]. As with the Pd microkinetic modeling study, it was ascribed to the higher activation barrier for the formation of toluene through the C−O bond cleavage than for the benzaldehyde formation.
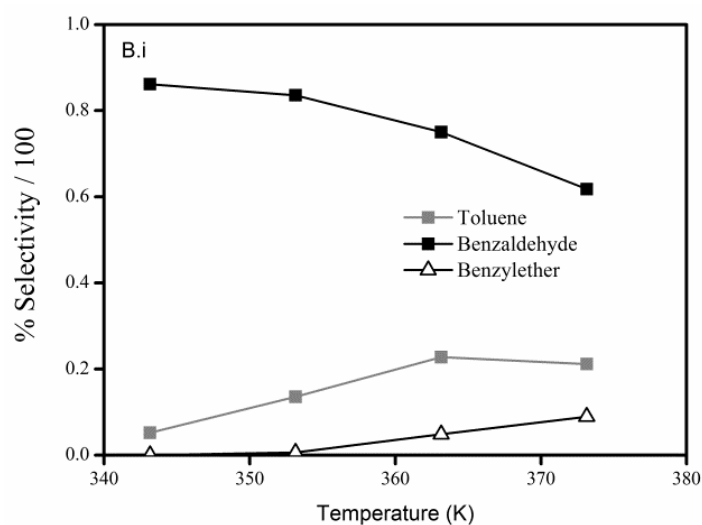
Figure 6. Selectivities as a function of the reactor temperature. Reprinted with permission from ref. [88]. Copyright 2014 WILEY-VCH Verlag GmbH & Co. KGaA, Weinheim.

3.2. Oxidant

Different oxidants have been used in the Pd catalyzed e BA oxidation, including air [90–92] and H_2O_2 [93,94]. However most of the studies have been performed using O_2 as oxidant [8]. Similar trends have been observed by most of these studies with an increased conversion and increased selectivity to benzaldehyde at higher O_2 pressures (this trend is further explained by the microkinetic modeling study described in the Section 4). For example, Cao et al. [88] showed that by varying the O_2 pressure from 2 to 5 bar, the conversion increased (78.5% and 95% at 2 and 5 bar, respectively) due to an increased O_2 solubility in the solution. Moreover, selectivity to benzaldehyde increased (57.7% and 77.8% at 2 and 5 bar, respectively) with a decreased in the amount of toluene formed (38.5% and 15.5% at 2 and 5 bar, respectively). The increased reaction rate at higher oxygen pressure has been also observed using Pd/AC as catalyst [86]. The authors correlated the trend with the proposed mechanism, discussed below, where the dissociation of BA is promoted by the oxygen. Higher oxygen pressure increased the selectivity to benzaldehyde suppressing the formation of toluene and ether (Figure 7).
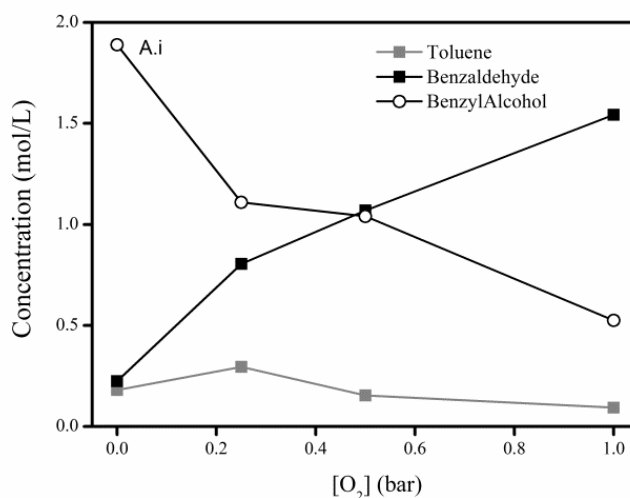
Figure 7. Product concentration as a function of the oxygen pressure. Reprinted with permission from ref. [88]. Copyright 2014 WILEY-VCH Verlag GmbH & Co. KGaA, Weinheim.

3.3. Concentration

As expected, under the conditions typically studied, higher alcohol concentration results in greater reaction rates but also results in changes in the selectivity. Some literature results will be summarized here, then the comprehensive kinetic models presented in Section 4. In one study, when increasing the concentration of BA from 0.0 to 5.5 M the BA conversion increased to reach the maximum at 1 M during the reaction over Pd/CN at 80 °C using toluene as solvent [82], while performing the reaction using higher concentrations lead to the diminishing of the BA conversion. Villa and coauthors investigated the effects of the alcohol concentration using a AuPd catalyst [41]. Carrying out the reaction at higher alcohol concentration over Au60-Pd40/AC, from 0.15 M to 1 M and in the presence of a base NaOH and for the same alcohol/metal (mol/mol) ratio, only a small change of TOF was obtained. For example, for an alcohol/metal ratio of 500 mol/mol the resulting TOF is 1000 h^{-1}, 1100 h^{-1}, 700 h^{-1} and 700 h^{-1} for a BA concentration of 0.15 M, 0.30 M, 0.60 M and 1 M, respectively. The above results suggests that the surface is largely covered with adsorbates during reaction, which is consistent with the kinetic simulations in reference, where simulations suggested that adsorbed oxygen was the dominant species under most conditions [95].

4. Mechanism and Microkinetic Models

An ideal goal of chemical research on catalysts involves understanding the mechanism and the kinetics at an elementary step level. Performing kinetic simulations of the mechanism and kinetics at an elementary step level is referred to as "microkinetic modelling". Until recently, there was no published mechanism detailed enough for microkinetic modeling. However, Savara et al. published a sufficiently complete mechanism and microkinetic model for benzylic alcohol oxidation over Pd/AC and AuPd/AC, [53,86,95] followed by a kinetic study by Galvanin et al. [89].

While there may be some mechanistic differences between Pd supported on carbon versus Pd supported on oxides, these recent studies suggest that the overall mechanism does not change greatly. Additionally, the mechanism does not change between Pd NPs and AuPd NPs, although the rate constants do change which results in changes in selectivity and activity. During early attempts to understand the source of toluene (mechanistically), Sankar et al. [96] interpreted data from AuPd/oxides as indicative of disproportionation of BA being the main source of toluene. However, the microkinetic modeling study by Savara et al. on Pd/AC indicated that a disproportionation reaction was not necessary to explain the presence of toluene. Instead, Savara et al.'s [86,95] model produced toluene with the same stoichiometry as a disproportionation reaction but via an alkyl intermediate formed by removal of the oxygen of alkoxy species formed from dissociative adsorption of the alcohol. It is worth noting that the model by Savara et al. explains not only the stoichiometry observed but also why the selectivity towards toluene is decreased when there is greater availability of surface oxygen in the system, which is also consistent with the earlier results of Sankar et al.

There are 6 different products that are observed from benzylic alcohol oxidation at 70–100 °C over Pd NPs: benzaldehyde, toluene, benzyl ether, benzene, benzoic acid and benzyl benzoate. A mechanism and microkinetic model that could explain how each of these products were formed, including the trends in selectivity with semi-quantitative prediction was published by Savara et al. [53,86,95]. The reduced equations of the relevant reaction steps can be summarized as follows, where "S" represents surface sites [53,86,95]. For simplicity in correlating the rate constants, the same numbering is retained for most of the equations as in the original publication.
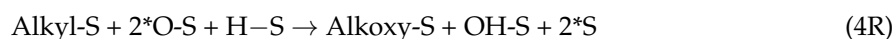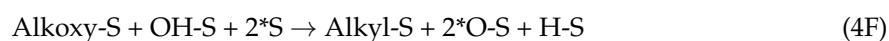
Oxygen and the alcohol each adsorb dissociatively on the surface, with the alcohol dissociation occurring towards an alkoxy and facilitated by a surface oxygen:
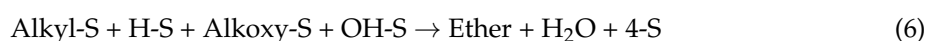
$$O_2 + 2S \rightarrow 2{*}O{-}S \tag{1}$$

$$Alcohol + S + O{-}S \rightarrow Alkoxy{-}S + OH{-}S \tag{2}$$
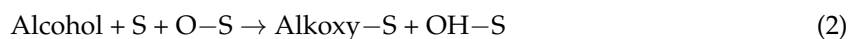
The alkoxy can dehydrogenate to form the aldehyde (this is the primary pathway and typically the most desired pathway).

$$Alkoxy{-}S + OH{-}S \rightarrow Aldehyde + H_2O + 2S \tag{3}$$
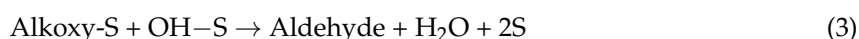
Alternatively, the alkoxy can lose an oxygen to create an alkyl state. The two states then exist in equilibrium, as shown in Equation (4F,R). In Equation (4F,R), we also show OH dissociating to H and S: but the H, O and OH concentrations are actually unknown. Thus, Equation (4F,R) and other Equations in this manuscript could be written differently: provided that the relevant elementary steps were retained, such as C$-$O bond breaking in step (4F) to form an oxygen on the surface and an alkyl species. Both Savara et al. and Galvanin et al. [95] assume that the H, O and OH species go on to make H_2O. (4R) was labelled as reaction 10 in the reference.

$$Alkoxy{-}S + OH{-}S + 2{*}S \rightarrow Alkyl{-}S + 2{*}O{-}S + H{-}S \tag{4F}$$

$$Alkyl{-}S + 2{*}O{-}S + H{-}S \rightarrow Alkoxy{-}S + OH{-}S + 2{*}S \tag{4R}$$
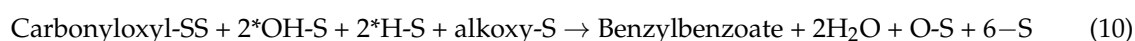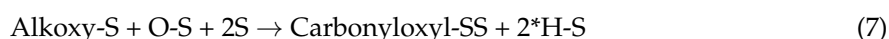
Once the alkyl group is formed, along with the surface hydrogen depicted in Equation (4), the equation to toluene and ether species are readily writable, with Equation (5) referred to as the "AT" step by Galvanin et al.:

$$Alkyl{-}S + H{-}S \rightarrow Toluene + 2S \tag{5}$$

$$Alkyl{-}S + H{-}S + Alkoxy{-}S + OH{-}S \rightarrow Ether + H_2O + 4{-}S \tag{6}$$

Equations (6) and (7) explain the correlated appearance of toluene and the ether as a function of conditions [86,95].

However, the benzoic acid, benzyl benzoate and benzene were all explained by the postulation of a carbonyloxyl intermediate (like a neutral carboxylate), which could explain the correlated appearance of these 3 species:

$$Alkoxy{-}S + O{-}S + 2S \rightarrow Carbonyloxyl{-}SS + 2{*}H{-}S \tag{7}$$

$$Carbonyloxyl{-}SS + OH{-}S + 2{*}H{-}S \rightarrow Benzene + CO_2 + H_2O + 5S \tag{8}$$

$$Carbonyloxyl{-}SS + OH{-}S + 2{*}H{-}S \rightarrow Benzoic\ Acid + H_2O + 5S \tag{9}$$

$$Carbonyloxyl{-}SS + 2{*}OH{-}S + 2{*}H{-}S + alkoxy{-}S \rightarrow Benzylbenzoate + 2H_2O + O{-}S + 6{-}S \tag{10}$$

Until the publication of this mechanism, the appearance of benzene was a mystery. The puzzle of benzene arose from the fact that it is a more hydrogenated species (relative to BA), yet was correlated with increasingly oxidizing conditions. The postulation of a carbonyloxyl intermediate explained this puzzle. The microkinetic modeling supported the existence of the carbonyloxyl intermediate.

Fitting of the data at multiple temperatures resulted in the rate constants and activation energies shown in Tables 1 and 2.

Table 1. Fitted Rate Constants from Microkinetic Model and Experimental Data at 70 °C [95].

k	Value
k1	8.2×10^{-5} s^{-1} Pa^{-1}
k2	1.4×10^{-1} s^{-1} mol^{-1} L
k3	5.1×10^{6} s^{-1}
k4	6.7×10^{8} s^{-1}
k5	4.4×10^{14} s^{-1}
k6	2.9×10^{11} s^{-1}
k7	1.6×10^{6} s^{-1}
k8	1.4×10^{14} s^{-1}
k9	5.5×10^{14} s^{-1}
k10	9.4×10^{12} s^{-1}
k11	2.2×10^{11} s^{-1}

Table 2. Fitted Values and Upper Limits for the Activation Energies (Ea) of Each Reaction, from Microkinetic Model and Experimental Data at 70–100 °C [95].

Ea	Fitted Value (kJ/mol)	Determined Upper Limit (kJ/mol)
Ea1	-	<130
Ea2	57.9	<90
Ea3	-	<120
Ea4	$0.96(\text{Ea}_{11}) + 12$	-
Ea5	129	<240
Ea6	175	<270
Ea7	-	<60
Ea8	-	<60
Ea9	-	<40
Ea10	-	<120
Ea11	$1.04(\text{Ea}_4) - 12$	-

Subsequently, the same microkinetic model was applied to AuPd/AC [53]. The main finding was that the selectivity differences between AuPd and Pd could be explained almost entirely due to differences in the strength of oxygen adsorption (Equation (1)), while the other rate constants were much less strongly affected. In that study, it was shown that greater oxygen pressures were required to push the reaction towards benzaldehyde when AuPd was used (relative to Pd). This aspect of the observed results and interpretation are consistent with the common knowledge that Au binds oxygen less strongly than Pd does and that suppression of the toluene route requires greater oxygen availability. However, other supports such as TiO_2 and other metal oxides may have greater oxygen availability during catalysis (potentially from on the oxide surface) and may thus result in different selectivity differences between Pd and AuPd.

The 2018 Galvanin kinetic study was performed with AuPd/TiO_2 [89]. The study did not look at products from the carbonyloxyl pathway but did attempt to understand the toluene/aldehyde selectivity and compared the kinetic model put forth by Savara et al. with kinetic models that alternatively involved a "direct" disproportionation reaction (between an alkoxy on the surface and an adsorbed alcohol, labelled DP) and a "hydrogenolysis" pathway (between a surface hydrogen and a surface alkoxy, labelled HL2). The HL2 pathway is stoichiometrically equivalent to the alkyl pathway proposed by Savara et al. and is thus not in conflict with the mechanism proposed by Savara et al. However, the existence of a direct DP pathway, as proposed by Galvanin et al., could not explain the appearance of the ether species being correlated with the toluene appearance (as observed by Savara et al.). Galvanin et al. did find in their simulations that oxygen would play a role similar to that found by Savara et al.: increased oxygen scavenges surface hydrogen and thus promotes formation of benzaldehyde through direct dehydrogenation and suppresses DP and HL2 (both of which require hydrogen in the Galvanin model). The Galvanin study concluded HL2 to be the

dominant pathway to toluene in their simulations, at $100-120$ °C, in contrasts to the AT step proposed by Savara et al. (Equation (5)). As noted, the HL2 pathway is stoichiometrically equivalent to the Savara et al. AT mechanism; with both proposals involving hydrogen in the step for toluene formation. Although Galvanin et al. were able to achieve a better fit by including a DP pathway, that model also involves a larger number of kinetic parameters and parallel pathways, which results in an easier fit but also increases the risk of overfitting. Thus, it is our view that it is unsettled whether AT or HL2 is the dominant pathway to toluene formation but that only the AT pathways explains the formation of the ether that has been observed and that the two pathways are stoichiomtrically equivalent. Interestingly, Galvanin et al. found a fitted value for the toluene producing rate constant of HL2 as having an optimum of 58.4 kJ/mol when it is assumed to be the dominant pathway to toluene, while Savara et al. find an optimal value of 129 kJ/mol for the AT step when assuming it is the dominant pathway. It is conceivable that studying the temperature dependence of toluene formation will enable discrimination between the AT and HL2 mechanisms. Galvanin et al. performed fittings with three models, including the model by Savara et al., in their study and found all three to be qualitatively similar (but found better quantitative agreement with the models that had more kinetic parameters and pathways than that of the Savara et al. model). Given the difficulty in controlling the uniformity of all variables (dispersion, particle size, support defects, etc.), the lack of knowledge of the reactions on the support, the lack of knowledge of adsorbate-adsorbate interactions and so forth, we currently take the interpretation that the model of Savara et al. is probably the correct model as it can predict all 6 products with the correct qualitative behavior. However, this model likely would need to be refined to include the additional complexities mentioned if greater quantitative agreement is desired, relative to experiment. In general, there is still room for additional detailed kinetic studies on this system but great care must be taken to try and control for these complexities noted (dispersion, particle size, support defects, etc.). Otherwise, experimental errors will be larger than the accuracy needed for the fits to tease out these factors and discriminate between the models proposed.

5. Summary

Benzylic alcohol oxidation over supported Palladium nanoparticles has been studied over the last 15 years resulting in greater than 50 publications. Early studies focused on the effects of morphology and particle size, determining that the most active particle size range appears to be between 2 and 6 nm, with some variation between studies as to what the most active particle size is. The support may play a role in this by modulating the electronic properties of the particle and also by stabilizing various particle sizes and dispersions. It was found that nitrogen incorporation into carbon supports greatly increased the stability and dispersion of the palladium nanoparticles. The activity and selectivity differences between oxide supports and carbon supports has been studied but requires greater study for quantitative understanding of these effects and to consider more types of supports. Alloying of gold and palladium has been shown to modulate the selectivity. In particular two studies (one on AuPd/AC and one on AuPd/oxides) utilized kinetic modelling to show that Au decreases the selectivity and activity for formation of benzaldehyde, which was explained by a decreased oxygen interaction with the catalyst surface. The addition of bismuth is believed to increase selectivity towards the aldehyde by suppressing the activity of high index Pd planes. Similar structural-suppression strategies have also been accomplished using other adsorbates, such as PVP. Detailed mechanistic studies and kinetic modeling have recently shown that the pathways to 6 different products (benzaldehyde, toluene, benzyl ether, benzene, benzoic acid and benzyl benzoate) can be explained by an alkoxy intermediate, an alkyl intermediate and, most interestingly, a minor pathway through a carbonyloxyl intermediate. Both a direct disproportionation mechanism and the alkyl pathway mechanism have been proposed for toluene formation. The proposed alkyl pathway mechanism explains the formation of benzyl ether and also the suppression of toluene formation when oxygen is more available on the surface. The extent of knowledge available relative to 15 years ago is much higher. The field is now poised for

more innovation in structural control, studies of support effects and potentially kinetic studies with increased accuracy and precision or across wider ranges of conditions.

References

1. Besson, M.; Gallezot, P. Selective oxidation of alcohols and aldehydes on metal catalysts. *Catal. Today* **2000**, *57*, 127–141. [CrossRef]

2. Davis, S.E.; Ide, M.S.; Davis, R.J. Selective oxidation of alcohols and aldehydes over supported metal nanoparticles. *Green Chem.* **2013**, *15*, 17–45. [CrossRef]

3. Parmeggiani, C.; Matassini, C.; Cardona, F. A step forward towards sustainable aerobic alcohol oxidation: New and revised catalysts based on transition metals on solid supports. *Green Chem.* **2017**, *19*, 2030–2050. [CrossRef]

4. Dhakshinamoorthy, A.; Asiri, A.M.; Garcia, H. Tuneable nature of metal organic frameworks as heterogeneous solid catalysts for alcohol oxidation. *Chem. Commun.* **2017**, *53*, 10851–10869. [CrossRef] [PubMed]

5. Sheldon, R.A. Recent advances in green catalytic oxidations of alcohols in aqueous media. *Catal. Today* **2015**, *247*, 4–13. [CrossRef]

6. Stahl, S.S. Palladium oxidase catalysis: Selective oxidation of organic chemicals by direct dioxygen-coupled turnover. *Angew. Chem. Int. Ed.* **2004**, *43*, 3400–3420. [CrossRef] [PubMed]

7. Schultz, M.J.; Sigman, M.S. Recent advances in homogeneous transition metal-catalyzed aerobic alcohol oxidations. *Tetrahedron* **2006**, *62*, 8227–8241. [CrossRef]

8. Mallat, T.; Baiker, A. Oxidation of alcohols with molecular oxygen on solid catalysts. *Chem. Rev.* **2004**, *104*, 3037–3058. [CrossRef] [PubMed]

9. Sheldon, R.A.; Kochi, J.K. *Metal Catalysed Oxidations of Organic Compounds*; Elsevier: Amsterdam, The Netherlands, 1981.

10. Joshi, S.R.; Kataria, K.L.; Sawant, S.B.; Joshi, J.B. Kinetics of oxidation of benzyl alcohol with dilute nitric acid. *Ind. Eng. Chem. Res.* **2005**, *44*, 325–333. [CrossRef]

11. Dimitratos, N.; Lopez-Sanchez, J.A.; Morgan, D.; Carley, A.; Prati, L.; Hutchings, G.J. Solvent free liquid phase oxidation of benzyl alcohol using Au supported catalysts prepared using a sol immobilization technique. *Catal. Today* **2007**, *122*, 317–324. [CrossRef]

12. Bowles, B.L.; Juneja, V.K. Inhibition of foodborne bacterial pathogens by naturally occurring food additives. *J. Food Saf.* **1998**, *18*, 101–112. [CrossRef]

13. Takeuchi, S.; Kochi, M.; Sakaguchi, K.; Nakagawa, K.; Mizutani, T. Benzaldehyde as a carcinostatic principle in figs. *Agric. Biol. Chem.* **1978**, *42*, 1449–1451.

14. Krings, U.; Berger, R.G. Biotechnological production of flavours and fragrances. *Appl. Microbiol. Biotechnol.* **1998**, *49*, 1–8. [CrossRef] [PubMed]

15. Alberici, F.; Pagani, L.; Ratti, G.; Viale, P. Ivermectin alone or in combination with benzyl benzoate in the treatment of human immunodeficiency virus-associated scabies. *Br. J. Dermatol.* **2000**, *142*, 969–972. [CrossRef] [PubMed]

16. Marx, S.; Baiker, A. Beneficial interaction of gold and palladium in bimetallic catalysts for the selective oxidation of benzyl alcohol. *J. Phys. Chem. C* **2009**, *113*, 6191–6201. [CrossRef]

17. Riemer, D.; Mandaviya, B.; Schilling, W.; Götz, A.C.; Kühl, T.; Finger, M.; Das, S. CO_2-catalyzed oxidation of benzylic and allylic alcohols with DMSO. *ACS Catal.* **2018**, *8*, 3030–3034. [CrossRef]

18. Sheikhi, E.; Adib, M.; Karajabad, M.A.; Gohari, S.J.A. Sulfuric Acid-promoted oxidation of benzylic alcohols to aromatic aldehydes in dimethyl sulfoxide: An efficient metal-free oxidation approach. *Synlett* **2018**, *29*, 974–978. [CrossRef]

19. Kim, H.R.; Jung, J.H.; Kim, J.N.; Ryu, E.K. Oxidation of benzylic and secondary alco-hols using m-chloroperbenzoic acid/hydro-gen chloride/N,N-dimethylformamide system. *Synth. Commun.* **1990**, *20*, 637–640. [CrossRef]

20. Pagliaro, M.; Campestrini, S.; Ciriminna, R. Ru-based oxidation catalysis. *Chem. Soc. Rev.* **2005**, *34*, 837–845. [CrossRef] [PubMed]

21. Luzzio, F.A. The oxidation of alcohols by modified oxochromium(VI)-amine reagents. *Org. React.* **1998**, *53*. [CrossRef]

22. Tidwell, T.T. Oxidation of alcohols to carbonyl compounds via alkoxysulfonium ylides: The moffatt, swern, and related oxidations. In *Organic Reactions*; John Wiley & Sons, Inc.: Hoboken, NJ, USA, 1990; pp. 297–555, ISBN 0471264180.

23. Chan-Thaw, C.E.; Villa, A.; Katekomol, P.; Su, D.; Thomas, A.; Prati, L. Covalent triazine framework as catalytic support for liquid phase reaction. *Nano Lett.* **2010**, *10*. [CrossRef] [PubMed]

24. Chan-Thaw, C.E.; Villa, A.; Prati, L.; Thomas, A. Triazine-based polymers as nanostructured supports for the liquid-phase oxidation of alcohols. *Chem. A Eur. J.* **2011**, *17*. [CrossRef] [PubMed]

25. Chan-Thaw, C.E.; Villa, A.; Veith, G.M.; Kailasam, K.; Adamczyk, L.A.; Unocic, R.R.; Prati, L.; Thomas, A. Influence of periodic nitrogen functionality on the selective oxidation of alcohols. *Chem. An. Asian J.* **2012**, *7*. [CrossRef] [PubMed]

26. Mori, K.; Hara, T.; Mizugaki, T.; Ebitani, K.; Kaneda, K. Hydroxyapatite-supported palladium nanoclusters: A highly active heterogeneous catalyst for selective oxidation of alcohols by use of molecular oxygen. *J. Am. Chem. Soc.* **2004**, *126*, 10657–10666. [CrossRef] [PubMed]

27. Yasu-eda, T.; Se-ike, R.; Ikenaga, N.; Miyake, T.; Suzuki, T. Palladium-loaded oxidized diamond catalysis for the selective oxidation of alcohols. *J. Mol. Catal. A Chem.* **2009**, *306*, 136–142. [CrossRef]

28. Dimitratos, N.; Villa, A.; Wang, D.; Porta, F.; Su, D.; Prati, L. Pd and Pt catalysts modified by alloying with Au in the selective oxidation of alcohols. *J. Catal.* **2006**, *244*. [CrossRef]

29. Enache, D.I. Solvent-free oxidation of primary alcohols to aldehydes using Au-Pd/TiO₂ catalysts. *Science* **2006**, *311*, 362–365. [CrossRef] [PubMed]

30. Li, G.; Enache, D.I.; Edwards, J.; Carley, A.F.; Knight, D.W.; Hutchings, G.J. Solvent-free oxidation of benzyl alcohol with oxygen using zeolite-supported Au and Au-Pd catalysts. *Catal. Lett.* **2006**, *110*, 7–13. [CrossRef]

31. Dimitratos, N.; Lopez-Sanchez, J.A.; Hutchings, G.J. Selective liquid phase oxidation with supported metal nanoparticles. *Chem. Sci.* **2012**, *3*, 20–44. [CrossRef]

32. Sheldon, R.; Arends, I.W.C.; Dijksman, A. New developments in catalytic alcohol oxidations for fine chemicals synthesis. *Catal. Today* **2000**, *57*, 157–166. [CrossRef]

33. Li, F.; Zhang, Q.; Wang, Y. Size dependence in solvent-free aerobic oxidation of alcohols catalyzed by zeolite-supported palladium nanoparticles. *Appl. Catal. A Gen.* **2008**, *334*, 217–226. [CrossRef]

34. Chen, J.; Zhang, Q.; Wang, Y.; Wan, H. Size-dependent catalytic activity of supported palladium nanoparticles for aerobic oxidation of alcohols. *Adv. Synth. Catal.* **2008**, *350*, 453–464. [CrossRef]

35. Zhou, Y.; Xiang, Z.; Cao, D.; Liu, C. Preparation and characterization of covalent organic polymer supported palladium catalysts for oxidation of CO and benzyl alcohol. *Ind. Eng. Chem. Res.* **2014**, *53*, 1359–1367. [CrossRef]

36. Ferri, D.; Mondelli, C.; Krumeich, F.; Baiker, A. Discrimination of active palladium sites in catalytic liquid-phase oxidation of benzyl alcohol. *J. Phys. Chem. B* **2006**, *110*, 22982–22986. [CrossRef] [PubMed]

37. Pang, S.H.; Román, A.M.; Medlin, J.W. Adsorption orientation-induced selectivity control of reactions of benzyl alcohol on pd(111). *J. Phys. Chem. C* **2012**, *116*, 13654–13660. [CrossRef]

38. Campisi, S.; Ferri, D.; Villa, A.; Wang, W.; Wang, D.; Kröcher, O.; Prati, L. Selectivity control in palladium-catalyzed alcohol oxidation through selective blocking of active sites. *J. Phys. Chem. C* **2016**, *120*, 14027–14033. [CrossRef]

39. Villa, A.; Ferri, D.; Campisi, S.; Chan-Thaw, C.E.; Lu, Y.; Kröcher, O.; Prati, L. Operando attenuated total reflectance FTIR spectroscopy: Studies on the different selectivity observed in benzyl alcohol oxidation. *ChemCatChem* **2015**, *7*, 2534–2541. [CrossRef]

40. Mondelli, C.; Ferri, D.; Grunwaldt, J.D.; Krumeich, F.; Mangold, S.; Psaro, R.; Baiker, A. Combined liquid-phase ATR-IR and XAS study of the Bi-promotion in the aerobic oxidation of benzyl alcohol over Pd/Al₂O₃. *J. Catal.* **2007**, *252*, 77–87. [CrossRef]

41. Villa, A.; Janjic, N.; Spontoni, P.; Wang, D.; Su, D.S.; Prati, L. Au-Pd/AC as catalysts for alcohol oxidation: Effect of reaction parameters on catalytic activity and selectivity. *Appl. Catal. A Gen.* **2009**, *364*, 221–228. [CrossRef]

42. Miedziak, P.; Sankar, M.; Dimitratos, N.; Lopez-Sanchez, J.A.; Carley, A.F.; Knight, D.W.; Taylor, S.H.; Kiely, C.J.; Hutchings, G.J. Oxidation of benzyl alcohol using supported gold-palladium nanoparticles. *Catal. Today* **2011**, *164*, 315–319. [CrossRef]

43. Moreno, I.; Dummer, N.F.; Edwards, J.K.; Alhumaimess, M.; Sankar, M.; Sanz, R.; Pizarro, P.; Serrano, D.P.; Hutchings, G.J. Selective oxidation of benzyl alcohol using in situ generated H2O2 over hierarchical Au–Pd titanium silicalite catalysts. *Catal. Sci. Technol.* **2013**, *3*, 2425. [CrossRef]

44. Peneau, V.; He, Q.; Shaw, G.; Kondrat, S.A.; Davies, T.E.; Miedziak, P.; Forde, M.; Dimitratos, N.; Kiely, C.J.; Hutchings, G.J. Selective catalytic oxidation using supported gold-platinum and palladium-platinum nanoalloys prepared by sol-immobilisation. *Phys. Chem. Chem. Phys.* **2013**, *15*, 10636–10644. [CrossRef] [PubMed]

45. Morad, M.; Sankar, M.; Cao, E.; Nowicka, E.; Davies, T.E.; Miedziak, P.J.; Morgan, D.J.; Knight, D.W.; Bethell, D.; Gavriilidis, A.; et al. Solvent-free aerobic oxidation of alcohols using supported gold palladium nanoalloys prepared by a modified impregnation method. *Catal. Sci. Technol.* **2014**, *4*, 3120–3128. [CrossRef]

46. Villa, A.; Wang, D.; Dimitratos, N.; Su, D.; Trevisan, V.; Prati, L. Pd on carbon nanotubes for liquid phase alcohol oxidation. *Catal. Today* **2010**, *150*, 8–15. [CrossRef]

47. Dimitratos, N.; Lopez-Sanchez, J.A.; Morgan, D.; Carley, A.F.; Tiruvalam, R.; Kiely, C.J.; Bethell, D.; Hutchings, G.J. Solvent-free oxidation of benzyl alcohol using Au-Pd catalysts prepared by sol immobilisation. *Phys. Chem. Chem. Phys.* **2009**, *11*, 5142–5153. [CrossRef] [PubMed]

48. Wang, D.; Villa, A.; Porta, F.; Prati, L.; Su, D. Bimetallic gold/palladium catalysts: Correlation between nanostructure and synergistic effects. *J. Phys. Chem. C* **2008**, *112*. [CrossRef]

49. He, Q.; Miedziak, P.J.; Kesavan, L.; Dimitratos, N.; Sankar, M.; Lopez-Sanchez, J.A.; Forde, M.M.; Edwards, J.K.; Knight, D.W.; Taylor, S.H.; et al. Switching-off toluene formation in the solvent-free oxidation of benzyl alcohol using supported trimetallic Au-Pd-Pt nanoparticles. *Faraday Discuss.* **2013**, *162*, 365–378. [CrossRef] [PubMed]

50. Villa, A.; Wang, D.; Spontoni, P.; Arrigo, R.; Su, D.; Prati, L. Nitrogen functionalized carbon nanostructures supported Pd and Au-Pd NPs as catalyst for alcohols oxidation. *Catal. Today* **2010**, *157*, 89–93. [CrossRef]

51. Enache, D.I.; Barker, D.; Edwards, J.K.; Taylor, S.H.; Knight, D.W.; Carley, A.F.; Hutchings, G.J. Solvent-free oxidation of benzyl alcohol using titania-supported gold-palladium catalysts: Effect of Au-Pd ratio on catalytic performance. *Catal. Today* **2007**, *122*, 407–411. [CrossRef]

52. Silva, T.A.G.; Teixeira-Neto, E.; López, N.; Rossi, L.M. Volcano-like behavior of Au-Pd core-shell nanoparticles in the selective oxidation of alcohols. *Sci. Rep.* **2014**, *4*, 5766. [CrossRef] [PubMed]

53. Savara, A.; Chan-Thaw, C.E.; Sutton, J.E.; Wang, D.; Prati, L.; Villa, A. Molecular origin of the selectivity differences between palladium and gld–palladium in benzyl alcohol oxidation: Different oxygen adsorption properties. *ChemCatChem* **2017**, *9*, 253–257. [CrossRef]

54. Tiruvalam, R.C.; Pritchard, J.C.; Dimitratos, N.; Lopez-Sanchez, J.A.; Edwards, J.K.; Carley, A.F.; Hutchings, G.J.; Kiely, C.J. Aberration corrected analytical electron microscopy studies of sol-immobilized Au + Pd, Au{Pd} and Pd{Au} catalysts used for benzyl alcohol oxidation and hydrogen peroxide production. *Faraday Discuss.* **2011**, *152*, 63–86. [CrossRef] [PubMed]

55. Villa, A.; Wang, D.; Veith, G.M.; Prati, L. Bismuth as a modifier of Au-Pd catalyst: Enhancing selectivity in alcohol oxidation by suppressing parallel reaction. *J. Catal.* **2012**, *292*, 73–80. [CrossRef]

56. Liu, X.Y.; Wang, A.; Zhang, T.; Mou, C.Y. Catalysis by gold: New insights into the support effect. *Nano Today* **2013**, *8*, 403–416. [CrossRef]

57. Villa, A.; Schiavoni, M.; Prati, L. Material science for the support design: A powerful challenge for catalysis. *Catal. Sci. Technol.* **2012**, *2*, 673–682. [CrossRef]

58. Prati, L.; Villa, A.; Lupini, A.R.; Veith, G.M. Gold on carbon: One billion catalysts under a single label. *Phys. Chem. Chem. Phys.* **2012**, *14*, 2969–2978. [CrossRef] [PubMed]

59. Karimi, B.; Abedi, S.; Clark, J.H.; Budarin, V. Highly efficient aerobic oxidation of alcohols using a recoverable catalyst: The role of mesoporous channels of SBA-15 in stabilizing palladium nanoparticles. *Angew. Chem. Int. Ed.* **2006**, *45*, 4776–4779. [CrossRef] [PubMed]

60. Qi, B.; Wang, Y.; Lou, L.L.; Huang, L.; Yang, Y.; Liu, S. Solvent-free aerobic oxidation of alcohols over palladium supported on MCM-41. *J. Mol. Catal. A Chem.* **2013**, *370*, 95–103. [CrossRef]

61. Hackett, S.F.J.; Brydson, R.M.; Gass, M.H.; Harvey, I.; Newman, A.D.; Wilson, K.; Lee, A.F. High-activity, single-site mesoporous Pd/Al$_2$O$_3$ catalysts for selective aerobic oxidation of allylic alcohols. *Angew. Chem. Int. Ed.* **2007**, *46*, 8593–8596. [CrossRef] [PubMed]

62. He, Y.; Yang, P.; Fan, J.; Liu, Y.; Du, Y.; Feng, J.; Fan, F.; Li, D. Facile and surfactant-free synthesis of supported Pd nanoparticles on hydrotalcite for oxidation of benzyl alcohol. *RSC Adv.* **2015**, *5*, 74907–74915. [CrossRef]

63. Qi, B.; Wang, Y.; Lou, L.-L.; Yang, Y.; Liu, S. Solvent-free aerobic oxidation of benzyl alcohol over palladium catalysts supported on MnO$_x$ prepared using an adsorption method. *React. Kinet. Mech. Catal.* **2012**, *108*, 519–529. [CrossRef]

64. Chen, L.; Yan, J.; Tong, Z.; Yu, S.; Tang, J.; Ou, B.; Yue, L.; Tian, L. Nanofiber-like mesoporous alumina supported palladium nanoparticles as a highly active catalyst for base-free oxidation of benzyl alcohol. *Microporous Mesoporous Mater.* **2018**, *266*, 126–131. [CrossRef]

65. Wang, H.; Kong, W.; Zhu, W.; Wang, L.; Yang, S.; Liu, F. One-step synthesis of Pd nanoparticles functionalized crystalline nanoporous CeO2and their application for solvent-free and aerobic oxidation of alcohols. *Catal. Commun.* **2014**, *50*, 87–91. [CrossRef]

66. Lu, Y.M.; Zhu, H.Z.; Liu, J.W.; Yu, S.H. Palladium nanoparticles supported on titanate nanobelts for solvent-free aerobic oxidation of alcohols. *ChemCatChem* **2015**, *7*, 4131–4136. [CrossRef]

67. Chen, Z.; Zou, P.; Zhang, R.; Dai, L.; Wang, Y. Nitrogen-incorporated SBA-15 mesoporous molecular sieve supported palladium for solvent-free aerobic oxidation of benzyl alcohol. *Catal. Lett.* **2015**, *145*, 2029–2036. [CrossRef]

68. Ji, R.; Zhai, S.; Zheng, W.; Xiao, Z.; An, Q.; Zhang, F. Enhanced metal-support interactions between Pd NPs and ZrSBA-15 for efficient aerobic benzyl alcohol oxidation. *RSC Adv.* **2016**, *6*, 70424–70432. [CrossRef]

69. Ji, R.; Zhai, S.-R.; Meng, Y.-Y.; Xiao, Z.-Y.; An, Q.-D. Deposition of N-doped carbon layers inside acidic ZrSBA-15: Significant enhancement of catalytic performance of Pd NPs toward benzyl alcohol aerobic oxidation. *J. Sol.-Gel Sci. Technol.* **2017**, *84*, 180–191. [CrossRef]

70. Zamani, F.; Hosseini, S.M. Palladium nanoparticles supported on Fe$_3$O$_4$/amino acid nanocomposite: Highly active magnetic catalyst for solvent-free aerobic oxidation of alcohols. *Catal. Commun.* **2014**, *43*, 164–168. [CrossRef]

71. Kong, L.; Wang, C.; Gong, F.; Zhu, W.; Zhong, Y.; Ye, X.; Li, F. Magnetic core–shell nanostructured palladium catalysts for green oxidation of benzyl alcohol. *Catal. Lett.* **2016**, *146*, 1321–1330. [CrossRef]

72. Wu, G.; Wang, X.; Guan, N.; Li, L. Palladium on graphene as efficient catalyst for solvent-free aerobic oxidation of aromatic alcohols: Role of graphene support. *Appl. Catal. B Environ.* **2013**, *136–137*, 177–185. [CrossRef]

73. Kandziolka, M.V.; Kidder, M.K.; Gill, L.; Wu, Z.; Savara, A. Aromatic-hydroxyl interaction of an alpha-aryl ether lignin model-compound on SBA-15, present at pyrolysis temperatures. *Phys. Chem. Chem. Phys.* **2014**, *16*, 24188–24193. [CrossRef] [PubMed]

74. Al-Marri, A.H.; Khan, M.; Shaik, M.R.; Mohri, N.; Adil, S.F.; Kuniyil, M.; Alkhathlan, H.Z.; Al-Warthan, A.; Tremel, W.; Tahir, M.N.; Khan, M.; Siddiqui, M.R.H. Green synthesis of Pd@graphene nanocomposite: Catalyst for the selective oxidation of alcohols. *Arab. J. Chem.* **2016**, *9*, 835–845. [CrossRef]

75. Rostamnia, S.; Doustkhah, E.; Karimi, Z.; Amini, S.; Luque, R. Surfactant-exfoliated highly dispersive Pd-supported graphene oxide nanocomposite as a catalyst for aerobic aqueous oxidations of alcohols. *ChemCatChem* **2015**, *7*, 1678–1683. [CrossRef]

76. Ravat, V.; Nongwe, I.; Coville, N.J. Palladium-supported boron-doped hollow carbon spheres as catalysts for the solvent-free aerobic oxidation of alcohols. *ChemCatChem* **2012**, *4*, 1930–1934. [CrossRef]

77. Arrigo, R.; Wrabetz, S.; Schuster, M.E.; Wang, D.; Villa, A.; Rosenthal, D.; Girsgdies, F.; Weinberg, G.; Prati, L.; Schlögl, R.; Su, D.S. Tailoring the morphology of Pd nanoparticles on CNTs by nitrogen and oxygen functionalization. *Phys. Chem. Chem. Phys.* **2012**, *14*. [CrossRef] [PubMed]

78. Hao, Y.; Wang, S.; Sun, Q.; Shi, L.; Lu, A.H. Uniformly dispersed Pd nanoparticles on nitrogen-doped carbon nanospheres for aerobic benzyl alcohol oxidation. *Cuihua Xuebao/Chin. J. Catal.* **2015**, *36*, 612–619. [CrossRef]

79. Luo, J.; Peng, F.; Wang, H.; Yu, H. Enhancing the catalytic activity of carbon nanotubes by nitrogen doping in the selective liquid phase oxidation of benzyl alcohol. *Catal. Commun.* **2013**, *39*, 44–49. [CrossRef]

80. Chan-Thaw, C.E.; Villa, A.; Veith, G.M.; Prati, L. Identifying the role of N-heteroatom location in the activity of metal catalysts for alcohol oxidation. *ChemCatChem* **2015**, *7*. [CrossRef]

81. Wang, L.; Zhu, L.; Bing, N.; Wang, L. Facile green synthesis of Pd/N-doped carbon nanotubes catalysts and their application in Heck reaction and oxidation of benzyl alcohol. *J. Phys. Chem. Solids* **2017**, *107*, 125–130. [CrossRef]

82. Xu, J.; Shang, J.K.; Chen, Y.; Wang, Y.; Li, Y.X. Palladium nanoparticles supported on mesoporous carbon nitride for efficiently selective oxidation of benzyl alcohol with molecular oxygen. *Appl. Catal. A Gen.* **2017**, *542*, 380–388. [CrossRef]

83. Tan, H.T.; Chen, Y.; Zhou, C.; Jia, X.; Zhu, J.; Chen, J.; Rui, X.; Yan, Q.; Yang, Y. Palladium nanoparticles supported on manganese oxide-CNT composites for solvent-free aerobic oxidation of alcohols: Tuning the properties of Pd active sites using MnOx. *Appl. Catal. B Environ.* **2012**, *119–120*, 166–174. [CrossRef]

84. Yan, Y.; Chen, Y.; Jia, X.; Yang, Y. Palladium nanoparticles supported on organosilane-functionalized carbon nanotube for solvent-free aerobic oxidation of benzyl alcohol. *Appl. Catal. B Environ.* **2014**, *156–157*, 385–397. [CrossRef]

85. Yang, Z.W.; Zhao, X.; Li, T.J.; Chen, W.L.; Kang, Q.X.; Xu, X.Q.; Liang, X.X.; Feng, Y.; Duan, H.H.; Lei, Z.Q. Catalytic properties of palygorskite supported Ru and Pd for efficient oxidation of alcohols. *Catal. Commun.* **2015**, *65*, 34–40. [CrossRef]

86. Savara, A.; Chan-Thaw, C.E.; Rossetti, I.; Villa, A.; Prati, L. Benzyl alcohol oxidation on carbon-supported Pd nanoparticles: Elucidating the reaction mechanism. *ChemCatChem* **2015**, *6*, 3464–3473. [CrossRef]

87. Wu, H.; Zhang, Q.; Wang, Y. Solvent-free aerobic oxidation of alcohols catalyzed by an efficient and recyclable palladium heterogeneous catalyst. *Adv. Synth. Catal.* **2005**, *347*, 1356–1360. [CrossRef]

88. Cao, E.; Sankar, M.; Firth, S.; Lam, K.F.; Bethell, D.; Knight, D.K.; Hutchings, G.J.; McMillan, P.F.; Gavriilidis, A. Reaction and Raman spectroscopic studies of alcohol oxidation on gold-palladium catalysts in microstructured reactors. *Chem. Eng. J.* **2011**, *167*, 734–743. [CrossRef]

89. Galvanin, F.; Sankar, M.; Cattaneo, S.; Bethell, D.; Dua, V.; Hutchings, G.J.; Gavriilidis, A. On the development of kinetic models for solvent-free benzyl alcohol oxidation over a gold-palladium catalyst. *Chem. Eng. J.* **2018**, *342*, 196–210. [CrossRef]

90. Dell'Anna, M.M.; Mali, M.; Mastrorilli, P.; Cotugno, P.; Monopoli, A. Oxidation of benzyl alcohols to aldehydes and ketones under air in water using a polymer supported palladium catalyst. *J. Mol. Catal. A Chem.* **2014**, *386*, 114–119. [CrossRef]

91. Bai, X.F.; Ye, F.; Zheng, L.S.; Lai, G.Q.; Xia, C.G.; Xu, L.W. Hydrosilane and bismuth-accelerated palladium catalyzed aerobic oxidative esterification of benzylic alcohols with air. *Chem. Commun.* **2012**, *48*, 8592–8594. [CrossRef] [PubMed]

92. Gallezot, P. Selective oxidation with air on metal catalysts. *Catal. Today* **1997**, *37*, 405–418. [CrossRef]

93. Pritchard, J.; Kesavan, L.; Piccinini, M.; He, Q.; Tiruvalam, R.; Dimitratos, N.; Lopez-Sanchez, J.A.; Carley, A.F.; Edwards, J.K.; Kiely, C.J.; Hutchings, G.J. Direct synthesis of hydrogen peroxide and benzyl alcohol oxidation using Au-Pd catalysts prepared by sol immobilization. *Langmuir* **2010**, *26*, 16568–16577. [CrossRef] [PubMed]

94. Sheldon, R.A.; Arends, I.W.C.E.; Ten Brink, G.J.; Dijksman, A. Green, catalytic oxidations of alcohols. *Acc. Chem. Res.* **2002**, *35*, 774–781. [CrossRef] [PubMed]

95. Savara, A.; Rossetti, I.; Chan-Thaw, C.E.; Prati, L.; Villa, A. Microkinetic modeling of benzyl alcohol oxidation on carbon-supported palladium nanoparticles. *ChemCatChem* **2016**, *8*, 2482–2491. [CrossRef]

96. Sankar, M.; Nowicka, E.; Tiruvalam, R.; He, Q.; Taylor, S.H.; Kiely, C.J.; Bethell, D.; Knight, D.W.; Hutchings, G.J. Controlling the duality of the mechanism in liquid-phase oxidation of benzyl alcohol catalysed by supported Au-Pd nanoparticles. *Chem. A Eur. J.* **2011**, *17*, 6524–6532. [CrossRef] [PubMed]